Received: 5 January 2021 | Revised: 18 April 2021 | Accepted: 7 May 2021

DOI: 10.1096/fj.202100017R

RESEARCH ARTICLE

THE FASEB JOURNAL

P38α-MAPK phosphorylates Snapin and reduces Snapin-mediated BACE1 transportation in APP-transgenic mice

Laura Schnöder[1,2] | Inge Tomic[1,2] | Laura Schwindt[1,2] | Dominic Helm[3] | Mandy Rettel[3] | Walter Schulz-Schaeffer[4] | Elmar Krause[5] | Jens Rettig[5] | Klaus Fassbender[1,2] | Yang Liu[1,2]

[1]Department of Neurology, Saarland University, Homburg/Saar, Germany

[2]German Institute for Dementia Prevention (DIDP), Saarland University, Homburg/Saar, Germany

[3]European Molecular Biology Laboratory, Proteomics Core Facility, Heidelberg, Germany

[4]Department of Neuropathology, Saarland University, Homburg/Saar, Germany

[5]Cellular Neurophysiology, Center for Integrative Physiology and Molecular Medicine (CIPMM), Saarland University, Homburg, Germany

Correspondence
Laura Schnöder and Yang Liu, Department of Neurology, Saarland University, Kirrberger Straße, Homburg/Saar 66421, Germany.
Email: Laura.Schnoeder@uks.eu (L. S.) and a.liu@mx.uni-saarland.de (Y. L.)

Funding information
This work was supported by the Alzheimer Forschung Initiative e.V. (#17046; to LS) and Deutsche Forschungsgemeinschaft (DFG) (LI1725/2-1; to Y. L.)

Abstract

Amyloid β peptide (Aβ) is the major pathogenic molecule in Alzheimer's disease (AD). BACE1 enzyme is essential for the generation of Aβ. Deficiency of p38α-MAPK in neurons increases lysosomal degradation of BACE1 and decreases Aβ deposition in the brain of APP-transgenic mice. However, the mechanisms mediating effects of p38α-MAPK are largely unknown. In this study, we used APP-transgenic mice and cultured neurons and observed that deletion of p38α-MAPK specifically in neurons decreased phosphorylation of Snapin at serine, increased retrograde transportation of BACE1 in axons and reduced BACE1 at synaptic terminals, which suggests that p38α-MAPK deficiency promotes axonal transportation of BACE1 from its predominant locations, axonal terminals, to lysosomes in the cell body. In vitro kinase assay revealed that p38α-MAPK directly phosphorylates Snapin. By further performing mass spectrometry analysis and site-directed mutagenic experiments in SH-SY5Y cell lines, we identified serine residue 112 as a p38α-MAPK-phosphorylating site on Snapin. Replacement of serine 112 with alanine did abolish p38α-MAPK knockdown-induced reduction of BACE1 activity and protein level, and transportation to lysosomes in SH-SY5Y cells. Taken together, our study suggests that activation of p38α-MAPK phosphorylates Snapin and inhibits the retrograde transportation of BACE1 in axons, which might exaggerate amyloid pathology in AD brain.

KEYWORDS

Alzheimer's disease, BACE1, *mapk14*, phosphorylation, Snapin, trafficking

Abbreviations: AD, Alzheimer's disease; APP, Alzheimer's amyloid precursor protein; Aβ, amyloid β peptide; BACE1, β-site of APP cleaving enzyme 1; ct, control; Dctn1, dynactin subunit 1; GFP, green fluorescent protein; HDAC3, Histone deacetylase 3; kd, knock-down; ko, knock-out; p38α-MAPK, p38 mitogen-activated protein kinase type α; PS1, presenilin 1; PSD-95, postsynaptic density protein 95; SDS/PAGE, sodium dodecyl sulfate polyacrylamide gel electrophoresis; SNAP-25, synaptosome-associated protein 25; SNARE, soluble N-ethylmaleimide-sensitive-factor attachment receptor; tg, transgenic; wt, wild-type.

1 | INTRODUCTION

Alzheimer's disease (AD) is the main cause of dementia with very limited therapeutic options. The amyloid β peptide (Aβ) is a key pathogenic molecule in AD, which accumulates in the brain and injures neurons directly[1,2] and indirectly by triggering neurotoxic inflammation.[3] Aβ is produced after serial cleavage of Alzheimer's amyloid precursor protein (APP) by β- and γ-secretases. The β-site of APP cleaving enzyme 1 (BACE1) is the rate limiting secretase for Aβ generation.[4-6] Inhibition of BACE1 might serve as a therapeutic strategy for AD patients. p38α-mitogen activated protein kinase (MAPK), sensitive to stress stimuli, is activated in neurons and microglia in association with Aβ plaques and neurofibrillary tangles.[7-9] Recently, we observed that deletion of p38α-MAPK in neurons facilitates BACE1 degradation in lysosomes thereby attenuating cerebral Aβ load in APP-transgenic AD mice.[10]

However, the detailed mechanism through which p38α-MAPK deficiency promotes the lysosomal degeneration of BACE1 remains unclear. BACE1 is predominantly located at axonal terminals, while lysosomes are enriched in the soma. Does p38α-MAPK deficiency drive the transportation of BACE1 to lysosomes? Previous studies have shown that the transport of BACE1-laden endosomes from axons to the soma is impaired, which might lead to an accumulation of BACE1. The impaired transportation perhaps also stacks APP in late endosomes at synaptic terminals. As a result, Aβ production and deposition in the brain is enhanced.[11,12] Interestingly, over-expression of Snapin, a synaptosome-associated protein 25 (SNAP-25) binding protein, restores the defective axonal transport of BACE1 to lysosomes.[13] As a dynein motor adaptor, Snapin also regulates trafficking of BACE1[14,15] and other proteins, eg, the tyrosine kinase,[16] from the late endosomes to lysosomes in neurons. Thus, we hypothesized that p38α-MAPK might phosphorylate Snapin and regulate the retrograde transport of BACE1 in axons and further into lysosomes.

In our study, we deleted p38α-MAPK specifically in neurons of APP-transgenic mice. p38α-MAPK deficiency did decrease phosphorylation of Snapin, and reduce BACE1 proteins at axonal terminals in the brain. With mass spectrometry and in vitro kinase assay, we identified serine 112 as a potential p38α-MAPK-phosphorylating site on Snapin. Replacing serine 112 with alanine abolished p38α-MAPK deficiency-enhanced BACE1 degradation. Thus, our study suggested that p38α-MAPK activation contributes to AD pathogenesis by phosphorylating Snapin.

2 | METHODS

2.1 | Animals

APP-transgenic mice with deletion of p38α-MAPK were established in our previous study by cross-breeding between APP/PS1-transgenic, *mapk14*-floxed mice ($p38^{fl/fl}$), and *nex* gene promoter-driven Cre knock-in mice (Nex-Cre).[10,17] All mice were analyzed at nine months of age using our established protocols.[10,17] Animal experiments followed relevant national rules and permissions issued by the local research ethical committee (registration numbers: 40/2014 and 43/2017).

2.2 | Snapin phosphorylation assay and BACE1 quantification in the brain

Phosphorylation sites on Snapin were predicted by the online software "NetPhos 3.1 Server" (http://www.cbs.dtu.dk/services/NetPhos-3.1) and "Group-based prediction system" (http://gps.biocuckoo.org/online.php) using the query sequence with UniProt accession number of O95295.

Right brain hemispheres from $APP^{tg}p38^{fl/fl}Nex^{cre/wt}$ and $APP^{tg}p38^{fl/fl}Nex^{wt/wt}$ littermate mice were homogenized in buffer A (50 mM Tris/HCl [pH 7.5], 150 mM NaCl, 1% Triton-X100, 2 mM EDTA, 2 mM EGTA, 50 nM ocadaic acid, 5 mM sodiumpyrophosphate, 2 mM sodium vanadate, 50 mM NaF and 150 mM NaCl) supplemented with protease inhibitor cocktail (Merck KGaA, Darmstadt, Germany) and phosphatase inhibitors (500 mM EGTA, 50 nM ocadaic acid, 5 mM sodiumpyrophosphate, 2 mM sodium vanadate, 50 mM NaF; all from Merck KGaA). The post-nuclear lysate at 2 mg/mL was pre-cleared with Dynabeads M-280 sheep anti-rabbit IgG (cat. 11203D; Thermo Fisher Scientific, Darmstadt, Germany) for 1 hour, and then incubated overnight at 4°C with rabbit polyclonal antibody against Snapin (cat. 148002; Synaptic Systems, Göttingen, Germany; 1:30 dilution). The antibody-bound Snapin was pulled down by magnetic beads-conjugated second antibody for another 2 hours at 4°C. After thoroughly washing, the immunoprecipitated Snapin was detected with Western blotting using rabbit polyclonal antibodies against phospho-serine (cat. SAB5200086; Merck KGaA) and phosphorylated-threonine (cat. 9381; Cell Signaling Technology, Danvers, MA, USA). Total Snapin was detected with Snapin antibody (Synaptic Systems).

The brain homogenate was also detected with Western blot for BACE1 and β-actin using rabbit monoclonal antibodies (clone D10E5 and 13E5, respectively; Cell Signaling Technology).

2.3 | Immunohistological analysis of Snapin in the brain

Serial 50-μm-thick sagittal sections were cut from the paraffin-embedded left hemisphere and stained with Snapin antibody (Synaptic Systems). Z-stack images with a distance of 0.5 μm were taken from hippocampus under Zeiss AxioImager.Z2

microscope with 40× objective. The length of linear Snapin staining was measured with ImageJ plugin "Skeletonized 3D" as we previously did for a measurement of blood vessels.[18] The length of Snapin staining along axons and in the neuropil was normalized by the area of region of interest.

2.4 | Synaptosomal isolation from mouse brains

Synaptosomes were isolated from right hemispheres of $APP^{tg}p38^{fl/fl}Nex^{cre/wt}$ and $APP^{tg}p38^{fl/fl}Nex^{wt/wt}$ littermate mice according to published methods[19,20] with minor modifications. Briefly, brain tissues were homogenized in 10× volumes of sucrose buffer (2 mM HEPES, pH 7.4, 320 mM sucrose, 50 mM EDTA, 20 mM DTT) supplemented with protease inhibitor cocktail (Merck KGaA) and phosphatase inhibitors, and then centrifuged at 3000 *g* for 2 minutes. The supernatant was collected and again centrifuged at 9200 *g* for 20 minutes. After the supernatant containing cytosolic proteins was removed, the pellet was resuspended in 1 mL sucrose buffer and loaded on a gradient buffer constructed with 23% (4 mL), 10% (4 mL), and 3% (3 mL) of Percoll (cat. 17-0891-02; Merck KGaA). The gradient was centrifuged for 17 minutes at 10 500 rpm in SW41 rotor (Beckman Coulter, Sinsheim, Germany). The band between the 10% and 23% Percoll layers containing synaptosomes was collected and washed in PBS.

In the end, synaptosomes were resuspended in 50 µL of buffer A. To examine the quality of isolation experiment, the lysate of synaptosomes was detected for synaptic proteins with rabbit polyclonal antibodies against Grin2a and PSD-95 (cat. 4205, and 9212, respectively; Cell Signaling Technology), and cytosolic protein, HDAC3, with rabbit monoclonal antibody (clone Y415; Novus biologicals, Wiesbaden, Germany). Thereafter, synaptosomal lysate was detected with rabbit polyclonal antibodies against p38-MAPK (cat. 9212; Cell Signaling Technology) and Snapin (Synaptic Systems), and with rabbit monoclonal antibody against BACE1 (clone D10E5; Cell Signaling Technology). Mouse monoclonal antibody against α-tubulin (clone DM1A; Abcam, Cambridge, United Kingdom) was used for a protein loading control.

2.5 | Culture of primary neurons and axonal trafficking assay

Primary neurons were cultured from the hippocampus and cortex of $p38^{fl/fl}Nex^{cre/wt}$ and $p38^{fl/fl}Nex^{cre/wt}$ embryos (E14 ± 0.5) with our established method.[17] After 7 days, cultured neurons were transfected with vectors encoding a fusion protein of BACE1 and monomeric green fluorescent protein (GFP) on C-terminus (kindly provided by S. Weihong, Centre for Brain Health, Vancouver, Canada)[21] in Lipofectamine 2000 (Thermo Fisher Scientific). Ten hours after transfection, the trafficking of BACE1-GFP in neuronal processes was measured with time-lapse imaging in a chamber at 37°C and filled with 5% CO_2 under Zeiss LSM 780 confocal microscopy (Göttingen, Germany). A total of 60 frames of time-lapse sequences were collected at 5-seconds intervals. The argon laser was used with 1% of intensity to minimize laser-induced bleaching of fluorescence and injury of cells. ImageJ with plugin MTrackJ was used to analyze the trafficking of BACE1.[22]

2.6 | In vitro kinase assay

We incubated 5.5 ng active p38α-MAPK kinase (cat. V2701; Promega GmbH, Walldorf, Germany), 150 µM ATP and recombinant human Snapin protein (cat. pro-663; ProSpec-Tany TechnoGene Ltd., Ness-Ziona, Israel) at increasing concentrations (0, 0.15, 0.24 and 0.3 µg/µL) for 60 minutes at RT in a white solid 96-well plate (cat. 3912; Corning GmbH, Wiesbaden, Germany). Thereafter, the ADP release from p38α-MAPK-mediated phosphorylation of Snapin was measured with ADP-Glo Kinase Assay (cat. V9101; Promega) on a luminescence reader, GloMax Navigator (Promega).

2.7 | Establishment of SH-SY5Y cell lines

p38α-MAPK knock-down cell lines (kd509 and kd709) as well as their control cells (kd-ct) were established in our previous study.[10] Snapin-overexpressing cell lines were constructed by stably transfecting SH-SY5Y cells with a pcDNA3.1+/C-(K)-DYK vector encoding human Snapin (OHu56032D) (wt) and vectors encoding Snapins containing point mutations from serine to alanine at 112 (S112A; AGT → GCC) and 133 (S133A; TCC → GCC) (all vectors were provided by GenScript, Leiden, the Netherlands). The over-expressed Snapin was tagged with FLAG at C-terminal. Thereafter, Snapin-overexpressed cell lines were further transfected with MAPK14 knock-down (709 kd) and control (kd-ct) vectors as described in our previous study.[10]

2.8 | Phosphorylation analysis with liquid chromatography electrospray ionization tandem mass spectrometry

FLAG-tagged Snapin was isolated from SH-SY5Y cells with and without *MAPK14* knock-down and purified with SDS/PAGE. The coomassie stained bands were cut from the gel and subjected to in-gel digestion with trypsin.[23] Peptides

were extracted from the gel pieces by sonication for 15 minutes, followed by centrifugation and supernatant collection. A solution of 50:50 water: acetonitrile, 1% formic acid (2 × the volume of the gel pieces) was added for a second extraction. The supernatant was pooled and processed using speed vacuum centrifugation. The samples were then dissolved in 10 µL of reconstitution buffer (96:4 water: acetonitrile, 1% formic acid) and analyzed by liquid chromatography electrospray ionization tandem mass spectrometry. An UltiMate 3000 RSLC nano LC system (Dionex; Thermo Fisher Scientific) fitted with a trapping cartridge (µ-Precolumn C18 PepMap 100, 5 µm, 300 µm i.d. × 5 mm, 100 Å) and an analytical column (nanoEase M/Z HSS T3 column 75 µm × 250 mm C18, 1.8 µm, 100 Å, Waters) was used. Trapping was carried out with a constant flow of trapping solvent (0.05% trifluoroacetic acid in water) at 30 µL/min onto the trapping column for 6 minutes. Subsequently, peptides were eluted and separated on the analytical column using a gradient composed of Solvent A (3% DMSO, 0.1% formic acid in water) and solvent B (3% DMSO, 0.1% formic acid in acetonitrile) with a constant flow of 0.3 µL/min. During the analytical separation, the percentage of solvent B was stepwise increased from 2% to 4% in 6 minutes, from 4% to 8% in 1 minute, then from 8% to 25% for a further 41 minutes and finally from 25% to 40% in another 5 minutes. The outlet of the analytical column was coupled directly to an Orbitrap Fusion Lumos (Thermo Fisher Scientific) mass spectrometer using the nanoFlex source. The peptides were introduced into the Orbitrap Fusion Lumos via a Pico-Tip Emitter 360 µm OD × 20 µm ID; 10 µm tip (New Objective) and an applied spray voltage of 2.4 kV, instrument was operated in a positive mode. The capillary temperature was set at 275°C. Full mass scans were acquired for a mass range 375-1200 m/z in profile mode in the orbitrap with resolution of 120 000. The filling time was set to a maximum of 50 microseconds with a limitation of 4e5 ions. The instrument was operated in a data-dependent acquisition (DDA) mode and MSMS scans were acquired in the Orbitrap with a resolution of 30 000, with a fill time of up to 86 microseconds and a limitation of 2e5 ions (AGC target). A normalized collision energy of 34 was applied. MS2 data was acquired in a profile mode. Acquired data was processed by IsobarQuant. As a search engine Mascot (v2.2.07) was used.[24] Data was searched against Uniprot *Homo sapiens* proteome database (UP000005640) containing common contaminants, reversed sequences and the sequences of the proteins of interest. The data was searched with the following modifications: Carbamidomethyl (C; fixed modification), Acetyl (N-term), Oxidation (M) and Phospho (STY) (variable modifications). The mass error tolerance for the full scan MS spectra was set to 10 ppm and for the MS/MS spectra to 0.02 Da. A maximum of two missed cleavages was allowed. For protein identification, a minimum of two unique peptides with a peptide length of at least seven amino acids and a false discovery rate below 0.01 were required on the peptide and protein level.

2.9 | Snapin phosphorylation assay in cultured SH-SY5Y cells

Cell lysate was prepared from SH-SY5Y cells over-expressing FLAG-tagged wild-type, and mutated (S112A or S133A) Snapins. Snapin proteins were purified with FLAG Immunoprecipitation Kit and the ANTI-FLAG M2 Affinity Gel (Sigma-Aldrich) according the manufacturer's instruction (Merck KGaA). The phosphorylation of FLAG-tagged Snapin was detected with Western blot using mouse monoclonal antibody against phospho-serine (clone PSR-45; Merck KGaA).

2.10 | β-secretase activity and protein assays in cultured SH-SY5Y cells

To measure β-secretase activity, membrane components were prepared from SH-SY5Y cells over-expressing wild-type and mutated Snapins with and without knockdown of p38α-MAPK expression.[25] Membrane components were incubated with fluorogenic substrate of β-secretase at 37°C (Merck KGaA). The fluorescence intensity in each well was measured for 73 cycles with intervals of 5 minutes with Synergy Mx Monochromator-based Multi-mode Microplate Reader (BioTek, Winooski, VT, USA). Fluorescence intensity of the first cycle was used as background. Membrane components were further lysed in buffer A, and detected with Western blot using BACE1 antibody (clone D10E5; Cell Signaling Technology).

2.11 | Subcellular fractionation by sucrose density gradient centrifugation

Subcellular fractions were prepared as described previously.[26,27] SH-SY5Y cells were harvested, washed with PBS and centrifuged at 300 *g* for 8 minutes. Cells were homogenized in TBS supplemented with protease inhibitor cocktail (Merck KGaA) by passaging 10 times through a 26-gauge needle. Nuclei and cell debris were removed by centrifugation at 1000 *g* for 10 minutes. The supernatant was transferred and centrifuged at 34 000 *g* for 15 minutes. The supernatant (S2), containing cytosolic proteins, was collected and used later as a purity control. The pellet was resuspended in 2 mL 45% sucrose in TBS and loaded on the bottom of a tube (cat. 344059; Beckman), which was overlaid by 6 mL 34.5% and 4 mL 14.3% sucrose buffer. After ultracentrifugation at 107 000 *g* for 12 hours, the cell lysate was separated into 12 fractions (1 mL per each) from the top to the bottom. For

Western blot analysis, all subcellular fractions with an equal volume were loaded onto PAGE gel and antibodies against LAMP1 (clone C54H11; Cell Signaling Technology), calnexin (cat. ab22595; Abcam) and α-tubulin (clone DM1A; Abcam) were used.

2.12 | Statistics

Data were presented as mean ± SEM. For multiple comparisons, we used one-way or two-way ANOVA followed by Bonferroni, Tukey, or Dunnett T3 *post hoc* test (dependent on the result of Levene's test to determine the equality of variances). Two independent-samples Student's *t* test was used to compare means for two groups of cases. All statistical analyses were performed with SPSS version 19.0 for Windows (IBM, New York, NY, USA). Statistical significance was set at $P < .05$.

3 | RESULTS

3.1 | Deletion of p38α-MAPK in neurons reduces Snapin phosphorylation in APP-transgenic mouse brain

We recently observed that deletion of p38α-MAPK in neurons decreases BACE1 in the brain of APP-transgenic mice.[10,17] At the beginning of this study, we re-confirmed our result by detecting BACE1 proteins in brains of $APP^{tg}p38^{fl/fl}Nex^{cre/wt}$ (p38α-MAPK deficient) and $APP^{tg}p38^{fl/fl}Nex^{wt/wt}$ (p38α-MAPK wild-type) littermate mice (Figure 1A; *t* test, $P < .05$). As Snapin potentially promotes the retrograde transportation and lysosomal degradation of BACE1,[2,14,28] we hypothesized that p38α-MAPK might phosphorylate Snapin and modify its function. Thus, we used NetPhosK 1.0 Server to predict the potential phosphorylation sites on Snapin using the UniProt accession number of O95295. p38α-MAPK potentially phosphorylates Snapin at serine sites 6, 10, 50, 112, 126 and 133, and at threonine sites 14 and 117.

We then immunoprecipitated Snapin from brain homogenates of p38α-MAPK-deficient and wild-type mice. We did observe that deletion of p38α-MAPK in neurons significantly decreased the phosphorylation level of Snapin at serines (Figure 1B; *t* test; $P < .05$), but not at threonines (Figure 1C; *t* test; $P > .05$).

3.2 | Deletion of p38α-MAPK in neurons reduces Snapin and BACE1 at axonal terminals in APP-transgenic mice

To investigate whether the reduced phosphorylation of Snapin changed the axonal transportation in p38α-MAPK-deficient mouse brain, we stained Snapin in hippocampi of $APP^{tg}p38^{fl/fl}Nex^{cre/wt}$ and $APP^{tg}p38^{fl/fl}Nex^{wt/wt}$ mice (Figure 2A). Interestingly, the length of Snapin antibody-stained linear structures was two-fold more in p38α-MAPK-deficient APP-transgenic mice (0.091 ± 0.004 μm) than in p38α-MAPK wild-type AD littermate mice (0.046 ± 0.004 μm) (Figure 2B; *t* test, $P < .001$). We divided Snapin-positive structures into different

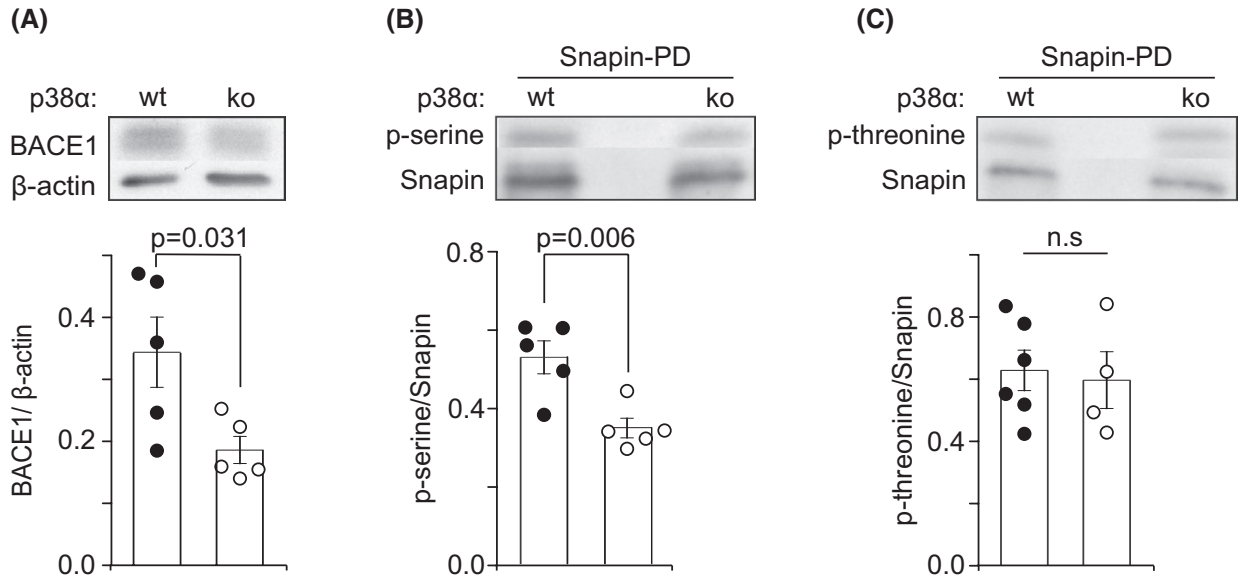

FIGURE 1 Deletion of p38α-MAPK in neurons reduces BACE1 and Snapin phosphorylation in APP-transgenic mice. Brain homogenates were prepared from 9-month-old APP-transgenic mice with (ko) and without (wt) deletion of p38α-MAPK in neurons. BACE1 was detected with Western blot (A; *t* test; n = 5 per group). Snapin was first pulled down and then detected with Western blot using antibodies against phospho-serine or phospho-threonine, and Snapin. The phosphorylation level of Snapin at serine was significantly decreased (B; *t* test; n = 5 per group), whereas the phosphorylation of Snapin at threonine was not changed by deletion of p38α-MAPK (C; *t* test; n > 4 per group)

groups according to their length (< 1, 1-5, 5-10 and >10 µm). Deletion of p38α-MAPK predominantly increased the percentages of long (5-10 and >10 µm) fragments (Figure 2C; two-way ANOVA, $P < .05$).

In following experiments, we isolated synaptosomes from the brain of $APP^{tg}p38^{fl/fl}Nex^{cre/wt}$ and $APP^{tg}p38^{fl/fl}Nex^{wt/wt}$ mice. The synaptosomal fraction was enriched with synaptic proteins, such as Grin2a, PSD95, and lack of cytosolic protein, HDAC3, indicating the success of our isolation experiments (Figure 2D). In synaptosomal fractions from $APP^{tg}p38^{fl/fl}Nex^{cre/wt}$ mice, the protein level of p38α-MAPK was about 72% lower than that in $APP^{tg}p38^{fl/fl}Nex^{wt/wt}$ mice (Figure 2E; *t* test, $P < .001$). Quantitative Western blot revealed that the protein level of Snapin decreased by 38% (Figure 2F; *t* test, $P < .001$) and that of BACE1 decreased by 51% (Figure 2G; *t* test, $P < .05$) in synaptosomes from p38α-MAPK-deficient APP-transgenic mice compared to p38α-MAPK-wild-type APP mice. Thus, deletion of p38α-MAPK appeared to drive Snapin and BACE1 to leave synaptic terminals.

3.3 | Deletion of p38α-MAPK increases BACE1 trafficking in primary cultured neurons

As we observed that p38α-MAPK deficiency re-located Snapin and BACE1 in the brain, we assumed that p38α-MAPK should regulate the trafficking of BACE1 in axons. We over-expressed a fusion protein of BACE1 and its C-terminal-tagged GFP

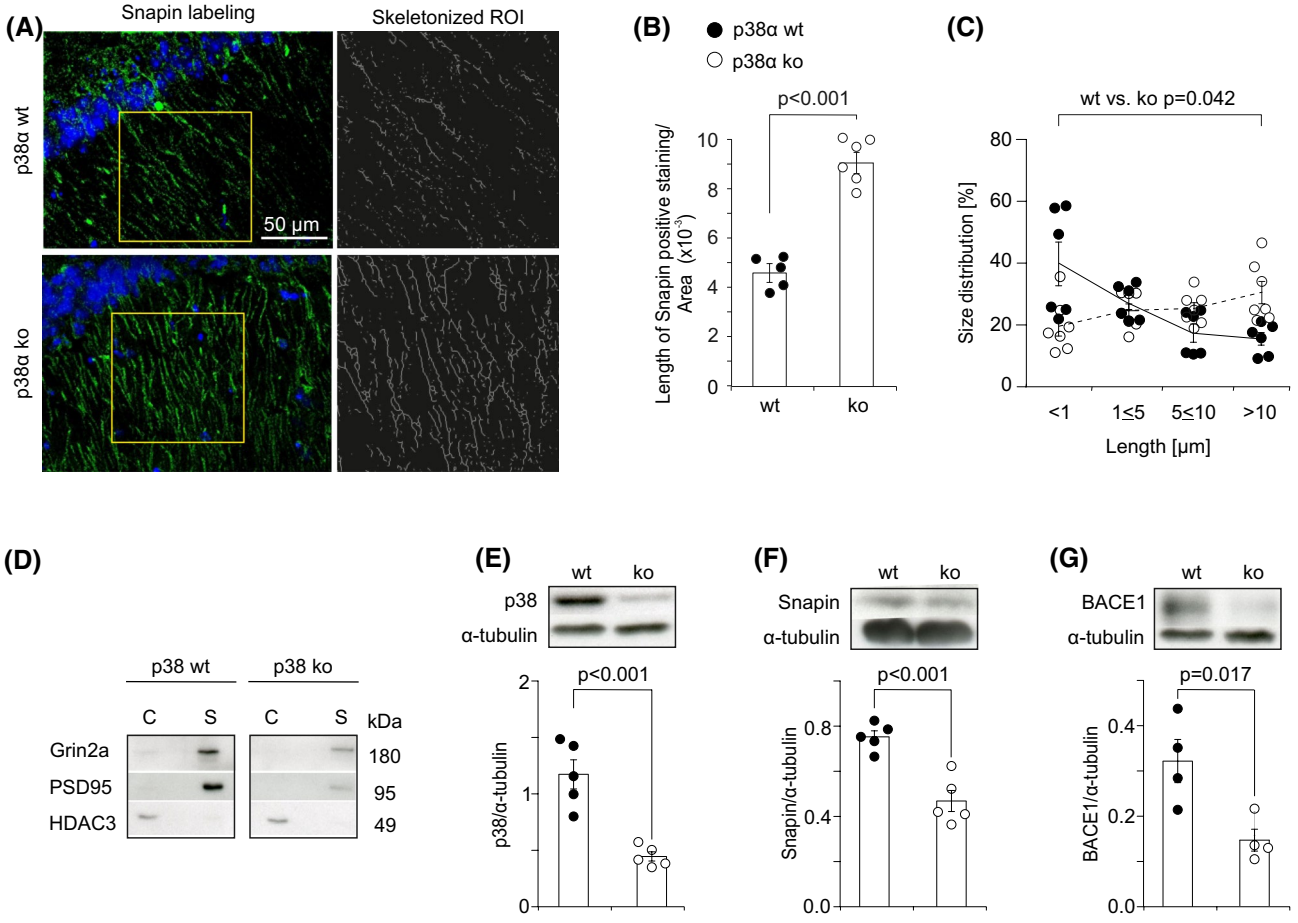

FIGURE 2 Deletion of p38α-MAPK in neurons re-locates Snapin and decreases Snapin and BACE1 in synaptosomes in APP-transgenic mice. Immunofluorescent labelling of Snapin was performed to evaluate the subcellular distribution of Snapin in 9-month-old APP-transgenic mice with (ko) and without (wt) deletion of p38α-MAPK in neurons (A). Snapin staining-positive neuronal processes in cropped region were skeletonized and measured for the length (A). The total length of Snapin antibodies—reactive processes adjusted by the area of region analyzed was significantly longer in p38α-MAPK ko mice than in p38α-MAPK wt mice (B; *t* test; n ≥ 5 per group). Binning analysis (C) revealed a higher proportion of short and lower proportions of long Snapin staining in p38α wt than p38α ko animals (two-way ANOVA; n ≥ 6 per group). Synaptosomes were further isolated from 9-month-old p38α-MAPK-ko and -wt APP-transgenic mice. Purity of isolated synaptosomes (S) was examined by detecting synaptosomal (Grin2a, PSD95) and cytoplasmic (HDAC3) proteins. Cytoplasmic fraction was used as a control (D). Thereafter, p38-MAPK, Snapin and BACE1 were quantitated in isolated synaptosomes with Western blot (E-G). Deletion of p38α-MAPK significantly decreased the protein levels of all 3 proteins tested. *t* test, n ≥ 4 per group

in p38α-MAPK-deficient and wild-type cultured neurons. Time-lapse images of neurons were taken under a confocal microscope. Serial frames of the image stack were depicted (Figure 3A,B). BACE1-GFP particles in p38α-MAPK wild-type neurons moved with significantly shorter distance (Figure 3C; wt: 4.68 ± 0.58 μm and ko: 17.68 ± 3.02 μm; *t* test, $P < .001$) and slower velocity (Figure 3D; wt: 6.96 ± 0.88 μm/min and ko: 33.88 ± 5.90 μm/min; *t* test, $P < .001$) than in p38α-MAPK-deficient neurons. Moreover, p38α-MAPK wild-type neurons displayed more stationary BACE1-GFP particles than p38α-MAPK-deficient neurons (Figure 3E; wt: 41.91 ± 3.35% of total particles and ko: 11.14 ± 3.98% of total particles; *t* test, $P < .001$). Thus, p38α-MAPK deficiency promoted the axonal transport of BACE1, which was in accordance with our observation in p38α-MAPK-deficient mouse brain.

3.4 | p38α-MAPK phosphorylated Snapin at serine residue 112

Our experiments described above suggested that p38α-MAPK regulated BACE1 transportation in axons potentially through phosphorylating Snapin. We directly incubated the recombinant p38α-MAPK and Snapin in the presence of ATP. As shown in Figure 4A, as the amount of Snapin used in the reaction increased, the conversion of ATP to ADP, as shown in luminance intensity, increased, indicating that p38α-MAPK can phosphorylate Snapin.

We used our previously constructed p38α-MAPK-knocked down (kd709 and kd509) and wild-type (kd-ct) SH-SY5Y cell lines.[10] The protein level of p38-MAPK was significantly decreased by knock-down of *MAPK14* gene (Figure 4B; one-way ANOVA; $P < .05$). We observed that deletion of p38α-MAPK significantly reduced phosphorylation of Snapin at serine by ~40% in kd709 and by ~50% in kd509 compared with kd-ct cells (Figure 4C; one-way ANOVA; $P < .05$). Deletion of p38α-MAPK altered neither phosphorylation at threonine nor the total amount of Snapin (data not shown).

We then constructed new SH-SY5Y cell lines overexpressing FLAG-tagged Snapin with (kd709) and without (kd-ct) knock-down of p38α-MAPK. We purified FLAG-tagged Snapin for mass spectrometry analysis. The sequence detected in several independently repeated experiments covered 58%-75% of Snapin sequence. The serines at position 112 (S112) and 133 (S133) were identified in p38α-MAPK wild-type cells (kd-ct) for the phosphorylation modification with a delta mod value >40 and a Mascot peptide score >32 (Figure 4D,E). Other identified serine and threonine sites with potential phosphorylation had either low Mascot peptide scores or small delta mod values, which indicated that these amino acids were not phosphorylated or their low phosphorylation levels were below the detection sensitivity of mass spectrometry.[29] Interestingly, in p38α-MAPK-deficient SH-SY5Y cells, the phosphorylation on S112 was undetectable, which strongly suggested that S112 was the phosphorylation site of p38α-MAPK.

To verify the finding from mass spectrometry analysis, we continued to constructed FLAG-tagged Snapin-transgenic SH-SY5Y cells, in which serine 112 (S112) or serine 133

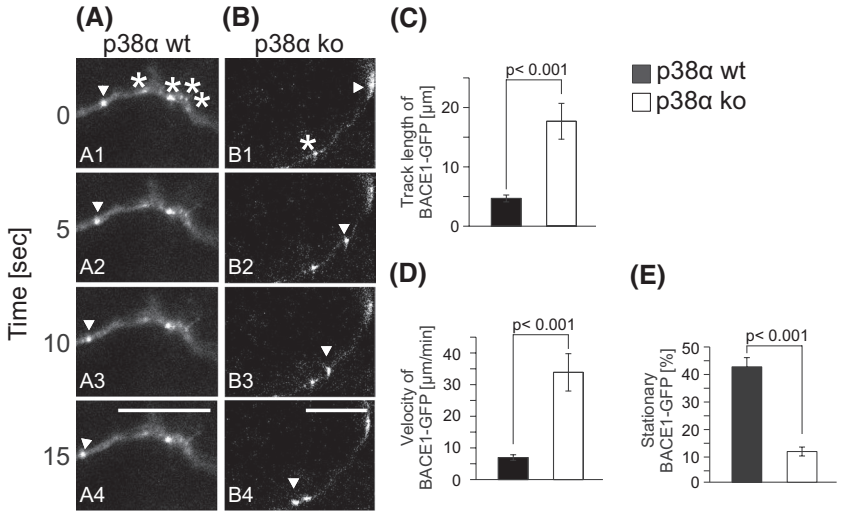

FIGURE 3 Deletion of p38α-MAPK promotes BACE1 trafficking in cultured neurons. BACE1-GFP fusion protein was expressed in hippocampal neurons cultured from p38α-MAPK-deficient (ko) and wild-type (wt) mice. Its trafficking was analyzed by serially imaging neurons under confocal microscopy with an interval of 5 seconds for total 60 frames. BACE1-GFP particles were followed along the axon in retrograde direction (p38α-MAPK wt: A1-A4, and ko: B1-B4; scale: 10 μm). The white arrowheads mark the traced BACE1-GFP particles over time and the asterisks in A1 and B1 mark stationary particles. The track length (C) and the velocity (D) of BACE1-GFP particles was significantly increased in p38α-MAPK ko neurons than in wt cells (*t* test; n ≥ 14 neurons and ≥68 particles per group). p38α-MAPK wt neurons showed significantly higher percentage of stationary BACE1-GFP particles (*t* test; n ≥ 6 neurons and ≥180 particles per group)

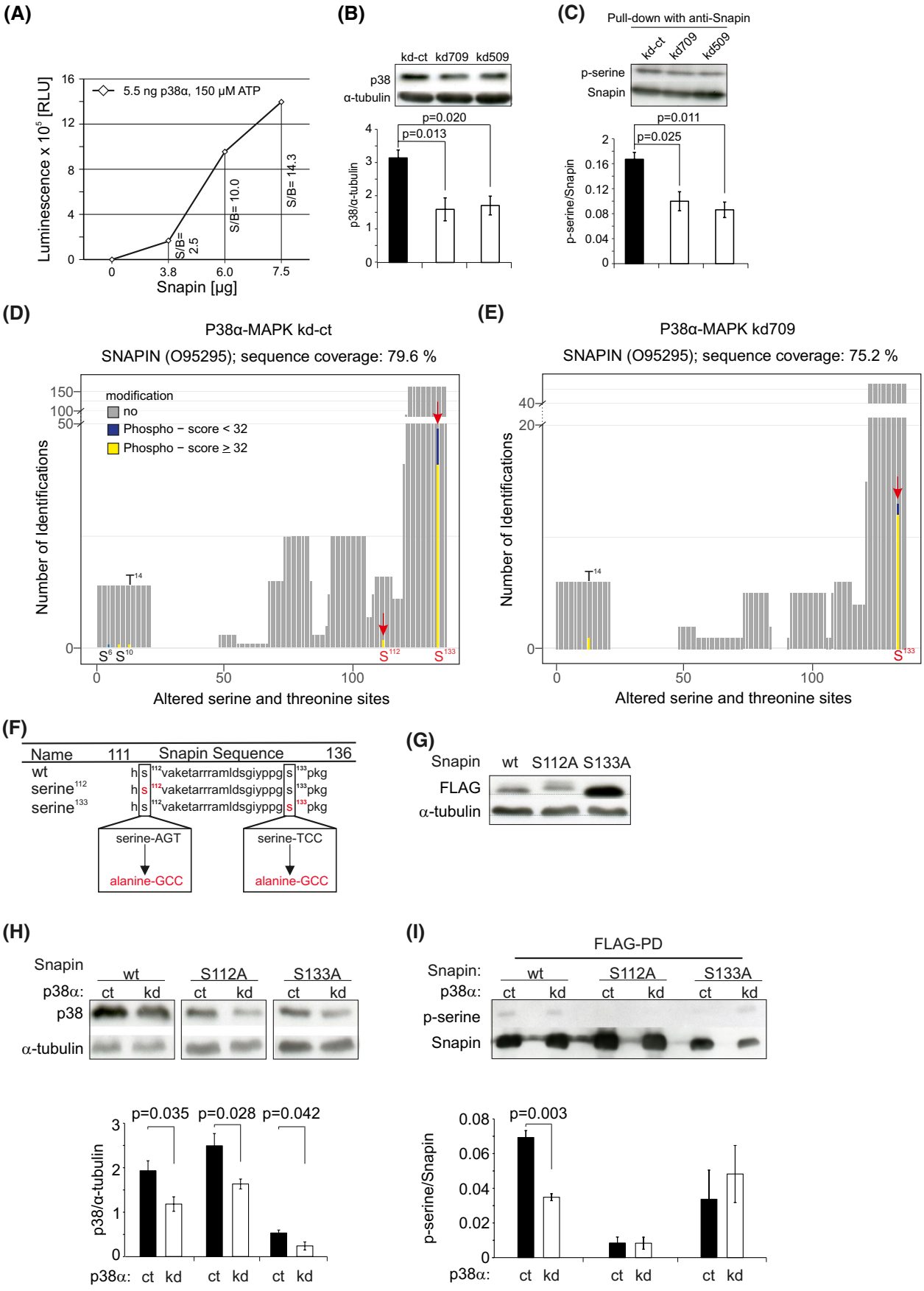
(A)
5.5 ng p38α, 150 µM ATP
Luminescence x 10^5 [RLU]
Snapin [µg]
S/B= 2.5
S/B= 10.0
S/B= 14.3
(B)
kd-ct kd709 kd509
p38
α-tubulin
p=0.020
p=0.013
p38/α-tubulin
(C)
Pull-down with anti-Snapin
kd-ct kd709 kd509
p-serine
Snapin
p=0.011
p=0.025
p-serine/Snapin
(D)
P38α-MAPK kd-ct
SNAPIN (O95295); sequence coverage: 79.6 %
modification
no
Phospho − score < 32
Phospho − score ≥ 32
Number of Identifications
Altered serine and threonine sites
(E)
P38α-MAPK kd709
SNAPIN (O95295); sequence coverage: 75.2 %
Number of Identifications
Altered serine and threonine sites
(F)
Name 111 Snapin Sequence 136
wt hs112vaketarrramldsgiyppgs133pkg
serine112 hs112vaketarrramldsgiyppgs133pkg
serine133 hs112vaketarrramldsgiyppgs133pkg
serine-AGT
alanine-GCC
serine-TCC
alanine-GCC
(G)
Snapin wt S112A S133A
FLAG
α-tubulin
(H)
Snapin
wt S112A S133A
p38α: ct kd ct kd ct kd
p38
α-tubulin
p=0.035 p=0.028 p=0.042
p38/α-tubulin
p38α: ct kd ct kd ct kd
(I)
FLAG-PD
Snapin: wt S112A S133A
p38α: ct kd ct kd ct kd
p-serine
Snapin
p=0.003
p-serine/Snapin
p38α: ct kd ct kd ct kd

FIGURE 4 p38α-MAPK phosphorylates Snapin at serine residue 112. In the in vitro kinase assay, 5.5 ng of recombinant p38α-MAPK was incubated with recombinant Snapin in the presence of 150 μM ATP. The conversion of ATP to ADP was shown in luminance intensity. The production of ADP increases with the amount of Snapin proteins used (A; shows results from one of the two independently repeated experiments). SH-SY5Y cells were stably transfected with p38α-MAPK knock-down (kd709, kd509) and control (kd-ct) vectors. The protein levels of p38-MAPK in kd709 and kd509 cells were ~50% of that in kd-ct cells (B; one-way ANOVA followed by Bonferroni *post hoc* test; n ≥ 3 per group). Snapin was pulled down from cell lysate with anti-Snapin antibody and detected with antibodies against phospho-serine. Knock-down of p38α-MAPK significantly attenuated Snapin phosphorylation in kd709 and kd509 cells compared with kd-ct controls (C; one-way ANOVA followed by Bonferroni *post hoc* test; n ≥ 3 per group). In following experiments, SH-SY5Y cell lines were constructed to over-express FLAG-tagged Snapin with and without knock-down of p38α-MAPK (kd709 and kd-ct, respectively). FLAG-tagged Snapin was isolated and purified for mass spectrometry analysis. The detected sequence covered >75% of whole sequence of Snapin. Sequenced amino acids were coded in grey (without modifications), blue (with minor phosphorylation; Mascot peptide score <32) and yellow (with high-level phosphorylation; Mascot peptide score ≥32). Serine sites S^{112} and S^{133} highlighted in red were detected in p38α-MAPK kd-ct cells with highest mascot peptide scores and delta mod values ≥20 (D). In p38α-MAPK kd709 cells, phosphorylation of S^{112} was undetectable (E). To verify the results from mass spectrometry analysis, new SH-SY5Y cell lines over-expressing wild-type (wt), and S112A or S133A-mutated FLAG-tagged Snapins with (kd709) and without (kd-ct) knock-down of p38α-MAPK were further constructed (F and G). The knock-down of p38α-MAPK led to similar reduction of p38-MAPK in Snapin wt, S112A and S133A cell lines (H; *t* test; n ≥ 3 per group). Finally, the immunoprecipitated FLAG-tagged Snapin was detected with phospho-serine-specific antibodies. Knock-down of p38α-MAPK significantly reduce phosphorylation of wt Snapin on serine residues (H, *t* test; n ≥ 3 per group). However, the phosphorylation was nearly undetectable on S112A-mutated Snapin and the phosphorylation of S133A-mutated Snapin was not altered by p38α-MAPK deficiency (I, *t* test; n ≥ 3 per group)

(S133) in Snapin was replaced with alanine (Figure 4F). These cell lines were further knocked down for the expression of p38α-MAPK. The expression of FLAG-tagged Snapins was detected with Western blot (Figure 4G). In various Snapin-expressing cell lines, p38α-MAPK proteins were similarly reduced (40%-50%) after transfection of knock-down vector (kd709) compared with transfection of control vector (kd-ct) (Figure 4H; *t* test; $P < .05$). With these cell lines, we again observed that deletion of p38α-MAPK inhibited the phosphorylation of wild-type Snapin at serine (Figure 4I; *t* test; $P = .003$); however, the serine phosphorylation was nearly undetectable in S112A-mutated FLAG-tagged Snapin with both knocked down and normal expression of p38α-MAPK in cells. In S133A-mutated FLAG-tagged Snapin, p38α-MAPK deficiency even tended to increase the phosphorylation at serine. These experiments supported that p38α-MAPK phosphorylates Snapin at residue S112.

3.5 | S112A mutation on Snapin abolished p38α-MAPK-induced protein reduction and lysosomal distribution of BACE1 in SH-SY5Y cells

As Snapin regulates trafficking of BACE1[14,15] from endosomes to lysosomes in neurons, we assumed that the over-expressed mutated Snapin should interfere with the endogenous Snapin in the regulation of BACE1 levels and subcellular localization. We measured β-secretase activity and proteins in the membrane components prepared from SH-SY5Y cells. In SH-SY5Y cells over-expressing FLAG-tagged wild-type Snapin, p38α-MAPK deficiency reduced both the activity and protein of BACE1 (Figure 5A,B; *t* test; $P < .05$), which corroborated our previous observation.[10] However, in SH-SY5Y cells over-expressing S112A-mutated Snapin, knock-down of p38α-MAPK changed neither activity nor proteins of BACE1. Moreover, in SH-SY5Y cells over-expressing S133A-mutated Snapin, p38α-MAPK deficiency decreased the activity and protein level of BACE1, with a stronger effect than in wild-type Snapin-expressed cells (Figure 5A,B; *t* test; $P < .05$).

In further experiments, we detected BACE1 in subcellular fractions. The lysosome marker, LAMP1, was enriched in fraction 5 and 10. As fraction 5 was also positive for calnexin, a protein of endoplasmic reticulum, we considered fraction 10 as the fraction of lysosomes (Figure 5C,D). The cytoskeleton protein, α-tubulin, was absent in all subcellular fractions and only detectable in the cytosolic supernatant S2. We detected BACE1 proteins and quantified its relative amount in all fractions. When calculating the ratio of BACE1 amount in the lysosomal fraction (No. 10) among the total BACE1 protein in all subcellular fractions, we observed that p38α-MAPK deficiency increased the distribution of BACE1 in the lysosomal fraction in wild-type Snapin-expressing cells (Figure 5E-G; 3.1 ± 0.6% vs 12.7 ± 2.6% in p38α-MAPK-wildtype and knocked down cells, respectively; *t* test, $P < .05$), which corroborates our previous finding.[10] However, in S112A-mutated Snapin-expressing cells, p38α-MAPK deficiency did not alter the distribution of BACE1 in lysosomes (Figure 5H-J; *t* test, $P > .05$). As a control, in S133A-mutated Snapin-expressing SH-SY5Y cells, deficiency of p38α-MAPK served the same effect on BACE1 distribution as in wild-type Snapin-expressing cells (Figure 5K-M; 3.6 ± 1.0% vs 7.3 ± 0.4% in p38α-MAPK-wildtype and knocked down cells, respectively; *t* test, $P < .05$). Thus, our results support that p38α-MAPK phosphorylates Snapin on S112 and subsequently inhibits the lysosomal distribution of BACE1 in neuronal cells.

4 | DISCUSSION

Axonal transport, especially retrograde transport, is damaged in AD at the early disease stage,[30,31] which forms an AD-hallmark of neuritic dystrophy.[32] We previously observed that deletion of p38α-MAPK in neurons promotes lysosomal BACE1 degradation and attenuates Aβ deposits in APP-transgenic mouse brain.[10] In this study, we further demonstrated that p38α-MAPK deficiency reduces phosphorylation of Snapin, which might facilitate the transport of BACE1 into lysosomes.

Snapin can be phosphorylated by various kinases such as casein kinase 1δ,[33] protein kinase A[34] and leucine-rich repeat kinase 2.[35] In our study, we identified p38α-MAPK as a new Snapin kinase, which is evidenced by the following

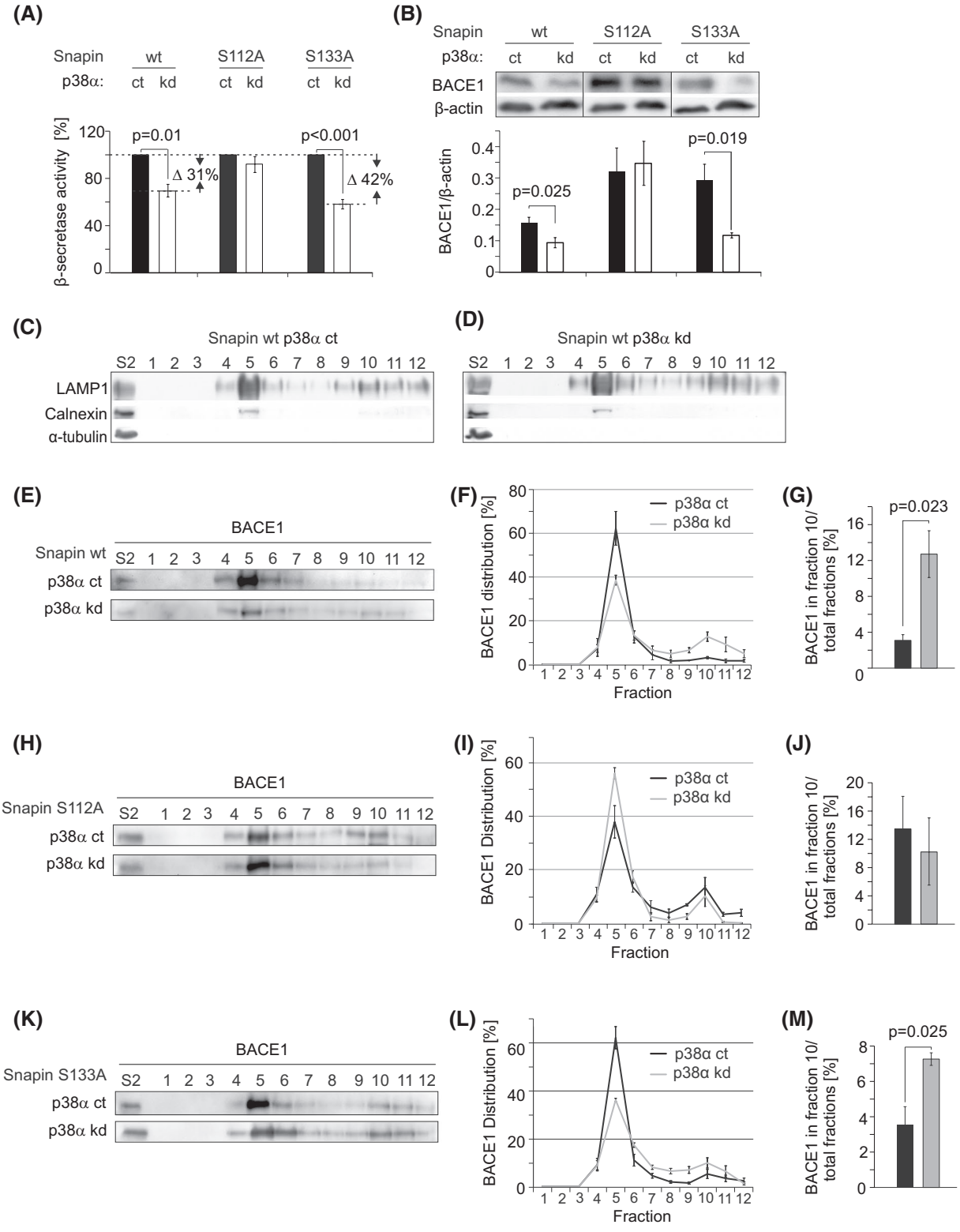

FIGURE 5 Replacement of serine 112 with alanine in Snapin abolishes p38α-MAPK deficiency-induced reduction of BACE1 activity and protein, and lysosomal transportation. Membrane components were prepared from p38α-MAPK-knocked down (kd) and wild-type (ct) SH-SY5Y cells over-expressing FLAG-tagged wild-type (wt), S112A or S133A-mutated Snapin. β-secretase activity was measured by incubating membrane components with fluorogenic β-secretase substrates at 37°C for 6 h. The protein level of BACE1 in isolated membrane components was determined by quantitative Western blot. Knock-down of p38α-MAPK significantly decreases both β-secretase activity and BACE1 protein in wt Snapin-overexpressing cells, however, alters neither in S112A-mutated Snapin-overexpressing cells (A and B; *t* test; $n \geq 3$ per group). In S133A-mutated Snapin-overexpressing cells, knock-down of p38α-MAPK significantly decreases both β-secretase activity and BACE1 protein even with stronger effects than in wt Snapin-overexpressing cells (A and B; *t* test; $n \geq 3$ per group). Subcellular fractions were prepared from wt, and S112A or S133A-mutated Snapin-overexpressing cells using sucrose density gradient centrifugation. Fraction no. 10 was enriched with LAMP1, but absent for calnexin and α-tubulin, as detected with Western blot, and then considered as the lysosomal fraction (C and D). Thereafter, subcellular fractions and cytosolic supernatant (S2) were immunoblotted for BACE1 (E, H and K). The amount of BACE1 in different subcellular fractions was quantified and the ratio of BACE1 in fraction 10 among the total BACE1 protein in all fractions was calculated (F, I and L). The distribution of BACE1 in lysosomal fraction was significantly increased by knocking down of p38α-MAPK in wt and S133A-mutated Snapin-overexpressing cells (E-G and K-M; *t* test; $n = 3$ per group), but not in S112A-mutated Snapin-overexpressing cells (H-J; *t* test, $P > .05$; $n = 3$ per group)

results: (a) deletion of p38α-MAPK in neurons decreases phosphorylation level of Snapin in APP-transgenic mice; (b) mass spectrometry analysis reveals phosphorylation at serine 112 (S112) on Snapin in p38α-MAPK wild-type SH-SY5Y cells, but not in p38α-MAPK-deficient cells; (c) replacement of S112 with alanine abolishes p38α-MAPK-mediated phosphorylation of Snapin and p38α-MAPK deficiency-induced reduction of BACE1 in SH-SY5Y cells; and (d) p38α-MAPK directly phosphorylates recombinant Snapin protein in an in vitro kinase assay. Our results are in accordance with a yeast two-hybrid screening experiment, which showed that p38α-MAPK likely binds to Snapin.[36]

It should be noted that phosphorylation of Snapin might inhibit its physiological function. For example, phosphorylation at threonine 117 by the leucine-rich repeat kinase 2 results in its lower binding to SNARE complex and impairs the exocytosis of vesicles.[32] Our examination on APP-transgenic mouse brain showed that deletion of p38α-MAPK increases the immuno-fluorescent staining of Snapin along axons and decreases protein levels of Snapin in synaptosomes, which suggests that the less phosphorylated Snapin is more active in the transportation of BACE1 from the axonal terminal to the soma. In cultured neurons, we did observe that p38α-MAPK deficiency promotes BACE1 trafficking along neuronal processes, although it remains unclear whether reduction of phosphorylation on Snapin is a driving force. To answer this question, we need to mask p38α-MAPK-phosphorylating sites (ie, S112) on Snapin in primary cultured neurons, which is technically difficult.

It has been reported that an efficient shipment of BACE1 from endosomes into lysosomes is necessary for a sufficient degradation of BACE1.[27] As a dynein motor adaptor, Snapin does regulate trafficking of BACE1[14,15] from the late endosomes to lysosomes in neurons. In SH-SY5Y cells, we over-expressed S112A-mutated Snapin, which deleted p38α-MAPK-mediated phosphorylation of Snapin. We did observe that p38α-MAPK deficiency-induced reduction of BACE1 proteins and its enhanced lysosomal distribution was abolished. Thus, p38α-MAPK might not only regulate axonal transportation but also affect Snapin-involved trafficking of proteins between subcellular organelles.

Besides phosphorylating Snapin, p38α-MAPK might also regulate axonal transportation of BACE1 through other mechanisms. Tau interacts with tubulin and stabilizes cytoskeleton under physiological conditions.[37-39] Tau becomes hyper-phosphorylated and detaches skeleton in AD, which impairs protein trafficking in axons.[40-44] Our recent study showed that deletion of p38α-MAPK prevents Tau from hyperphosphorylation in neurons.[17] We also observed that the transcription of dynein cofactor dynactin 1 (Dctn1) is up-regulated in p38a-MAPK-deficient APP-transgenic mice.[17] Silencing genes encoding dynein/dynactin complex was observed to block retrograde transport and exaggerate the axonal pathology in Tau-overexpressed *Drosophila*.[45] However, to clarify these potential mechanisms, we need further experiments.

Abnormal axonal transport, especially retrograde transport, and loss of axonal architecture are common features of axonopathies, not only in AD, but also in other neurodegenerative diseases, such as amyotrophic lateral sclerosis, Huntington's, and Parkinson's diseases. As Snapin serves as an adaptor protein of dynein in retrograde transport,[15] p38α-MAPK inhibition might also protect axons in various neurodegenerative diseases.

In our recent study, we observed that deficiency of p38α-MAPK inhibits NMDA receptor-mediated calcium influx and enhances the clearance of calcium from the cytosol of neurons, which might prevent calcium overload-induced neuronal death at AD lesion sites (eg, around Aβ deposits).[17] However, calcium is essential for the neuronal excitability, neurotransmitter release, and synaptic plasticity, under moderate concentrations.[46] Our previous studies revealed that Snapin enhances the association between synaptotagmin, a calcium-binding protein, and SNARE proteins, and facilitates the secretion of large dense-core vesicles from chromaffin cells.[47,48] Thus, p38α-MAPK deficiency might improve the neuronal function by activating Snapin in relatively healthy

brain regions in AD. The binding between Snapin and SNAP-25 requires the phosphorylation of Snapin at serine 50 by protein kinase A.[34] How p38α-MAPK-mediated phosphorylation regulates the function of Snapin and subsequent neuronal exocytosis needs a further investigation.

In summary, our studies showed that deletion of p38α-MAPK decreases phosphorylation of Snapin at serine residue 112 and enhances transportation of BACE1 from axonal terminals to lysosomes in the cell body, which might lead to BACE1 reduction and improve amyloid pathology in p38α-MAPK-deficient AD mice.[10,17] Our results contribute to a better understanding of molecular mechanisms underlying AD pathogenesis.

ACKNOWLEDGMENT

We thank Dr M. Jucker (Hertie Institute for Clinical Brain Research, Tübingen) for providing APP/PS1-transgenic mice; and Dr K. Nave (Max-Planck-Institute for Medicine, Göttingen) for Nex-Cre mice. The floxed-p38α-MAPK ($p38\alpha^{fl/fl}$) mice were kindly provided by Dr K. Otsu (Osaka University) though the RIKEN Bioresource Center. We thank Dr W. Song (The University of British Columbia, Vancouver) for providing BACE1-GFP vector. We appreciate Mirjam Göttel and Andrea Schottek for their excellent technical assistance.

CONFLICT OF INTEREST

The authors declare that they have no conflicts of interest with the contents of this article.

AUTHOR CONTRIBUTIONS

L. Schnöder and Y. Liu designed the research, acquired funding, and wrote the paper; L. Schnöder, I. Tomic, L. Schwindt, D. Helm, M. Rettel, and E. Krause performed the experiments; L. Schnöder, D. Helm, and M. Rettel analyzed the data; W. Schulz-Schaeffer, J. Rettig, and K. Fassbender contributed the analytic tools. All authors read and approved the final manuscript.

DATA AVAILABILITY STATEMENT

The data published in this study is available from the corresponding author.

REFERENCES

1. Shankar GM, Li S, Mehta TH, et al. Amyloid-β protein dimers isolated directly from Alzheimer's brains impair synaptic plasticity and memory. *Nat Med*. 2008;14:837.
2. Mucke L, Selkoe DJ. Neurotoxicity of amyloid beta-protein: synaptic and network dysfunction. *Cold Spring Harb Perspect Med*. 2012;2:a006338.
3. Hong S, Beja-Glasser VF, Nfonoyim BM, et al. Complement and microglia mediate early synapse loss in Alzheimer mouse models. *Science*. 2016;352:712-716.
4. Vassar R, Bennett BD, Babu-Khan S, et al. β-Secretase cleavage of Alzheimer's amyloid precursor protein by the transmembrane aspartic protease BACE. *Science*. 1999;286:735-741.
5. Yan R, Bienkowski MJ, Shuck ME, et al. Membrane-anchored aspartyl protease with Alzheimer's disease β-secretase activity. *Nature*. 1999;402:533-537.
6. Bodendorf U, Danner S, Fischer F, et al. Expression of human β-secretase in the mouse brain increases the steady-state level of β-amyloid. *J Neurochem*. 2002;80:799-806.
7. Hensley K, Floyd RA, Zheng N-Y, et al. p38 kinase is activated in the Alzheimer's disease brain. *J Neurochem*. 1999;72:2053-2058.
8. Akiyama H, Barger S, Barnum S, et al. Inflammation and Alzheimer's disease. *Neurobiol Aging*. 2000;21:383-421.
9. Zhu X, Rottkamp CA, Boux H, Takeda A, Perry G, Smith MA. Activation of p38 kinase links tau phosphorylation, oxidative stress, and cell cycle-related events in Alzheimer disease. *J Neuropathol Exp Neurol*. 2000;59:880-888.
10. Schnöder L, Hao W, Qin Y, et al. Deficiency of neuronal p38alpha MAPK attenuates amyloid pathology in Alzheimer disease mouse and cell models through facilitating lysosomal degradation of BACE1. *J Biol Chem*. 2016;291:2067-2079.
11. Buggia-Prevot V, Fernandez CG, Riordan S, et al. Axonal BACE1 dynamics and targeting in hippocampal neurons: a role for Rab11 GTPase. *Mol Neurodegener*. 2014;9:1.
12. Sadleir KR, Kandalepas PC, Buggia-Prevot V, Nicholson DA, Thinakaran G, Vassar R. Presynaptic dystrophic neurites surrounding amyloid plaques are sites of microtubule disruption, BACE1 elevation, and increased Abeta generation in Alzheimer's disease. *Acta Neuropathol*. 2016;132:235-256.
13. Feng T, Tammineni P, Agrawal C, Jeong YY, Cai Q. Autophagy-mediated regulation of BACE1 protein trafficking and degradation. *J Biol Chem*. 2017;292:1679-1690.
14. Ye X, Cai Q. Snapin-mediated BACE1 retrograde transport is essential for its degradation in lysosomes and regulation of APP processing in neurons. *Cell Rep*. 2014;6:24-31.
15. Cai Q, Lu L, Tian JH, Zhu YB, Qiao H, Sheng ZH. Snapin-regulated late endosomal transport is critical for efficient autophagy-lysosomal function in neurons. *Neuron*. 2010;68:73-86.
16. Zhou B, Cai Q, Xie Y, Sheng ZH. Snapin recruits dynein to BDNF-TrkB signaling endosomes for retrograde axonal transport and is essential for dendrite growth of cortical neurons. *Cell Rep*. 2012;2:42-51.
17. Schnöder L, Gasparoni G, Nordstrom K, et al. Neuronal deficiency of p38alpha-MAPK ameliorates symptoms and pathology of APP or Tau-transgenic Alzheimer's mouse models. *FASEB J*. 2020;34:9628-9649.
18. Decker Y, Muller A, Nemeth E, et al. Analysis of the vasculature by immunohistochemistry in paraffin-embedded brains. *Brain Struct Funct*. 2018;223:1001-1015.
19. Dunkley PR, Jarvie PE, Robinson PJ. A rapid Percoll gradient procedure for preparation of synaptosomes. *Nat Protoc*. 2008;3:1718-1728.
20. Ruan QT, Yazdani N, Blum BC, et al. A mutation in Hnrnph1 that decreases methamphetamine-induced reinforcement, reward, and dopamine release and increases synaptosomal hnRNP H and mitochondrial proteins. *J Neurosci*. 2020;40:107-130.
21. Qing H, Zhou W, Christensen MA, Sun X, Tong Y, Song W. Degradation of BACE by the ubiquitin-proteasome pathway. *FASEB J*. 2004;18:1571-1573.

22. Meijering E, Dzyubachyk O, Smal I. Methods for cell and particle tracking. In *Methods in Enzymology*, Vol. 504. Elsevier; 2012:183-200.
23. Savitski MM, Reinhard FB, Franken H, et al. Tracking cancer drugs in living cells by thermal profiling of the proteome. *Science*. 2014;346:1255784.
24. Franken H, Mathieson T, Childs D, et al. Thermal proteome profiling for unbiased identification of direct and indirect drug targets using multiplexed quantitative mass spectrometry. *Nat Protoc*. 2015;10:1567-1593.
25. Xie K, Liu Y, Hao W, et al. Tenascin-C deficiency ameliorates Alzheimer's disease-related pathology in mice. *Neurobiol Aging*. 2013;34:2389-2398.
26. Pasternak SH, Bagshaw RD, Guiral M, et al. Presenilin-1, nicastrin, amyloid precursor protein, and gamma-secretase activity are co-localized in the lysosomal membrane. *J Biol Chem*. 2003;278:26687-26694.
27. Kizuka Y, Kitazume S, Fujinawa R, et al. An aberrant sugar modification of BACE1 blocks its lysosomal targeting in Alzheimer's disease. *EMBO Mol Med*. 2015;7:175-189.
28. Ye X, Feng T, Tammineni P, et al. Regulation of synaptic amyloid-beta generation through BACE1 retrograde transport in a mouse model of Alzheimer's disease. *J Neurosci*. 2017;37:2639-2655.
29. Marx H, Lemeer S, Schliep JE, et al. A large synthetic peptide and phosphopeptide reference library for mass spectrometry-based proteomics. *Nat Biotechnol*. 2013;31:557-564.
30. Tammineni P, Cai Q. Defective retrograde transport impairs autophagic clearance in Alzheimer disease neurons. *Autophagy*. 2017;13:982-984.
31. Tammineni P, Ye X, Feng T, Aikal D, Cai Q. Impaired retrograde transport of axonal autophagosomes contributes to autophagic stress in Alzheimer's disease neurons. *eLife*. 2017;6:e21776.
32. Lee S, Sato Y, Nixon RA. Lysosomal proteolysis inhibition selectively disrupts axonal transport of degradative organelles and causes an Alzheimer's-like axonal dystrophy. *J Neurosci*. 2011;31:7817-7830.
33. Wolff S, Stoter M, Giamas G, et al. Casein kinase 1 delta (CK1delta) interacts with the SNARE associated protein snapin. *FEBS Lett*. 2006;580:6477-6484.
34. Chheda MG, Ashery U, Thakur P, Rettig J, Sheng Z-H. Phosphorylation of Snapin by PKA modulates its interaction with the SNARE complex. *Nat Cell Biol*. 2001;3:331-338.
35. Yun HJ, Park J, Ho DH, et al. LRRK2 phosphorylates Snapin and inhibits interaction of Snapin with SNAP-25. *Exp Mol Med*. 2013;45:e36.
36. Wang J, Yuan Y, Zhou Y, et al. Protein interaction data set highlighted with human Ras-MAPK/PI3K signaling pathways. *J Proteome Res*. 2008;7:3879-3889.
37. Caceres A, Kosik KS. Inhibition of neurite polarity by tau antisense oligonucleotides in primary cerebellar neurons. *Nature*. 1990;343:461-463.
38. Drubin DG, Kirschner MW. Tau protein function in living cells. *J Cell Biol*. 1986;103:2739-2746.
39. Weingarten MD, Lockwood AH, Hwo SY, Kirschner MW. A protein factor essential for microtubule assembly. *Proc Natl Acad Sci USA*. 1975;72:1858-1862.
40. Alonso A, Zaidi T, Novak M, Grundke-Iqbal I, Iqbal K. Hyperphosphorylation induces self-assembly of tau into tangles of paired helical filaments/straight filaments. *Proc Natl Acad Sci U S A*. 2001;98:6923-6928.
41. Alonso AC, Grundke-Iqbal I, Iqbal K. Alzheimer's disease hyperphosphorylated tau sequesters normal tau into tangles of filaments and disassembles microtubules. *Nat Med*. 1996;2:783-787.
42. Grundke-Iqbal I, Iqbal K, Quinlan M, Tung YC, Zaidi MS, Wisniewski HM. Microtubule-associated protein tau. A component of Alzheimer paired helical filaments. *J Biol Chem*. 1986;261:6084-6089.
43. Alonso Adel C, Mederlyova A, Novak M, Grundke-Iqbal I, Iqbal K. Promotion of hyperphosphorylation by frontotemporal dementia tau mutations. *J Biol Chem*. 2004;279:34873-34881.
44. Sengupta A, Kabat J, Novak M, Wu Q, Grundke-Iqbal I, Iqbal K. Phosphorylation of tau at both Thr 231 and Ser 262 is required for maximal inhibition of its binding to microtubules. *Arch Biochem Biophys*. 1998;357:299-309.
45. Butzlaff M, Hannan SB, Karsten P, et al. Impaired retrograde transport by the Dynein/Dynactin complex contributes to Tau-induced toxicity. *Hum Mol Genet*. 2015;24:3623-3637.
46. Berridge MJ, Bootman MD, Lipp P. Calcium–a life and death signal. *Nature*. 1998;395:645-648.
47. Schmidt T, Schirra C, Matti U, Stevens DR, Rettig J. Snapin accelerates exocytosis at low intracellular calcium concentration in mouse chromaffin cells. *Cell Calcium*. 2013;54:105-110.
48. Tian JH, Wu ZX, Unzicker M, et al. The role of Snapin in neurosecretion: snapin knock-out mice exhibit impaired calcium-dependent exocytosis of large dense-core vesicles in chromaffin cells. *J Neurosci*. 2005;25:10546-10555.

How to cite this article: Schnöder L, Tomic I, Schwindt L, et al. P38α-MAPK phosphorylates Snapin and reduces Snapin-mediated BACE1 transportation in APP-transgenic mice. *The FASEB Journal*. 2021;35:e21691. https://doi.org/10.1096/fj.202100017R